COOLING OF MICROPROCESSORS USING FLOW BOILING OF CO2 IN A MICRO-EVAPORATOR: PRELIMINARY ANALYSIS AND PERFORMANCE COMPARISONS

Cheng L.* and Thome J.R.
*Author for correspondence
Laboratory of Heat and Mass Transfer (LTCM),
Faculty of Engineering Science,
École Polytechnique Fédérale de Lausanne (EPFL),
Station 9, Lausanne, CH-1015,
Switzerland,
E-mail: lixincheng@hotmail.com, john.thome@epfl.ch

ABSTRACT

The flow pattern based flow boiling heat transfer and two-phase pressure drop models for CO_2, recently developed by Cheng et al. [1, 2], have been used to predict the thermal performance of CO_2 in a silicon multi-microchannel evaporator (67 parallel channels with a width of 0.223 mm, a height of 0.68 mm and a length of 20 mm) used for cooling of micro-processors. First, some simulation results of CO_2 flow boiling heat transfer and two-phase pressure drops in micro-scale channels are presented. The effects of channel diameter, mass flux, saturation temperature and heat flux on flow boiling heat transfer coefficients and two-phase pressure drops are addressed. Then, simulations of the base temperatures of the silicon multi-microchannel evaporator using R236fa and CO_2 evaporation were performed for the following conditions: base heat fluxes q_b = 20-100 W/cm^2, mass flux G = 987.6 kg/m^{2}s and saturation temperature T_{sat} = 25°C. It shows that the base temperatures using CO_2 are much lower than those using R236fa. Compared to R236fa, CO_2 has much higher heat transfer coefficients and lower pressure drops in the multi-microchannel evaporator. However, the operation pressure of CO_2 is much higher than that of R236fa. Based on the analysis and comparison, CO_2 appears to be a promising coolant for microprocessors at low operating temperatures but also presents a great technological challenge like other new cooling technologies.

INTRODUCTION

Advances in micro-electronics technology continue to develop with surprisingly rapidity and the energy density of electronic devices to be dissipated is becoming much higher. Thus, the thermal emission delivered from micro-electronic elements and components is still increasing considerably. Therefore, it is essential to develop new high heat flux cooling technology to meet the challenging heat dissipation requirements.

With the rapid miniaturization of devices to nanoscale and microscale, the new technologies taking advantage of these advances are faced with very serious heat dissipation problems per unit volume (cooling CPUs and power electronics). The main issues in future trends for cooling of microprocessors are to dissipate footprint heat fluxes as high as 300 W/cm^2 or more while maintaining the chip safely below its maximum working temperature (less than 85°C) and providing a nearly uniform chip base temperature, the whole with a minimal energy consumption. This means that the conventional cooling technology, i.e. air cooling, will no longer be able to satisfy these heat duties. New solutions must be found to solve this problem. One possible solution is to use forced vaporization in micro-channels (multi-channels made of silicon or copper which may be used in copper cooling elements attached to CPUs in stacked CPUs, or directly in the silicon chip itself) by making use of the high heat transfer performance of two-phase flows [3-10]. In this aspect, flow boiling of low pressure refrigerants in multi-channel evaporators is a promising technique. The recent experimental results of high heat flux flow boiling of two refrigerants R236fa and R245fa in silicon multi-microchannels by our laboratory have shown very good heat transfer behaviors [9, 10].

To further explore the use of environmentally friendly refrigerants for the cooling of micro-processors, the present paper presents analysis of cooling of microprocessors using flow boiling of CO_2 in a silicon multi-microchannel evaporator. CO_2 is a natural refrigerant and has been intensively

investigated for automobile air-conditioning, refrigeration and heat pump systems over the past decade [1, 2, 11-13]. New flow pattern based heat transfer and pressure drop models for CO_2 evaporation have been recently developed in our laboratory for use in the design of micro-channel evaporators in automobile air-conditioning systems [1, 2] and are improvements of our previous models [12-13]. These models accurately predicted heat transfer coefficients, flow patterns and pressure drops over a wide range of conditions, including tube diameters from 0.6 to 10.06 mm. Especially, these models predicted the heat transfer and pressure drops in both single and multi micro-channels.

In the present study, our recent models for CO_2 [1, 2] have been used to predict the thermal performance of CO_2 evaporation in a silicon multi-microchannel evaporator (67 parallel channels with a width of 0.223 mμm, a height of 0.68 mm and a length of 20 mm). This geometry was chosen since we have recent test data for such a test section with a low pressure refrigerant R236fa [9]. First, some simulated results of CO_2 flow boiling heat transfer and two-phase pressure drops in micro-scale channels are presented for various conditions. The effects of channel diameter, mass flux, saturation temperature and heat flux on flow boiling heat transfer coefficients and two-phase pressure drops are analyzed. Then, simulations of base temperatures of the silicon multi-microchannel evaporator, comparing R236fa and CO_2 evaporation, have been performed for the following conditions: base heat fluxes q_b = 20-100 W/cm^2, mass flux G = 987.6 kg/m^{2}s and saturation temperature T_{sat} = 25°C, and the simulated results are compared and analyzed.

NOMENCLATURE

A	[m^2]	Channel cross section area
D	[m]	Channel diameter
e	[m]	Thickness of channel base
G	[kg/m^{2}s]	Mass flux
g	[m/s^2]	Gravitational acceleration
H	[m]	Channel height
h	[W/m^{2}K]	Heat transfer coefficient
i	[J/kg]	Latent heat of vaporization
k	[W/mK]	Thermal conductivity
L	[m]	Channel length
m	[1/m]	Parameter in Eq. (9)
N	[-]	Channel number
p	[Pa]	Pressure
q	[W/m^2]	Heat flux
T	[K]	Temperature
t	[m]	Channel wall thickness
W	[m]	Channel width
x	[-]	Vapor quality
z	[m]	distance along flow direction in the channel

Special characters

Δp	[Pa]	Pressure drop
ΔT	[K]	Temperature difference
ε	[-]	Void fraction
η	[-]	Fin efficiency
ρ	[kg/m^3]	Density
σ	[N/m]	Surface tension

Subscripts

a	Acceleration
b	Base
eq	Equivalent
f	Frictional
h	Hydraulic
in	Inlet
L	Liquid
out	Outlet
sat	saturation
si	Silicon
sub	Subcooled
$total$	total
V	Vapor
W	Wall
z	At z distance

SILICON MULTI-MICORCHANNEL EVAPORATOR AND PHYSICAL PROPERTIES OF R236FA AND CO_2

Geometry of Silicon Multi-Microchannel Evaporator

Figure 1 shows the schematic of the silicon multi-microchannel heat sink investigated in the present paper. It consists of 67 microchannels. The dimensions of the microchannels are the same as those of Agostini et al. [9, 10] and are given in Table 1, where the hydraulic diameter and equivalent diameter are defined as

$$D_h = \frac{2WH}{W + H} \tag{1}$$

$$D_{eq} = \sqrt{\frac{4A}{\pi}} = \sqrt{\frac{4WH}{\pi}} \tag{2}$$

The physical model is described as follows: (i) the bottom of the heat sink is uniformly heated by electric heating at a base heat flux q_b, (ii) the top of the heat sink is adiabatic, (iii) the coolant (CO_2 or R236fa) flows in the silicon multi-microchannel evaporator without inlet subcooling, ΔT_{sub} = 0 K. With these conditions, the base temperature T_b will be simulated using CO_2 and R236fa evaporation in the silicon microchannel evaporator at some operational conditions and the simulated results compared.
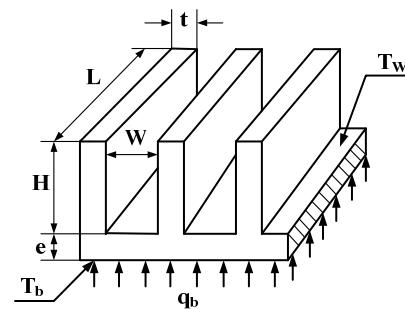

Figure 1 Schematic of a silicon multi-microchannel evaporator used for chips cooling.

Table 1 Channel dimensions

L (mm)	H (mm)	W (mm)	t (mm)	e (mm)	N	D (mm)
20	0.68	0.223	0.08	0.32	67	0.336* 0.44**

∗ hydraulic diameter and ∗∗equivalent diameter.

Physical Properties of R236fa and CO_2

Table 2 shows a comparison of the selected physical properties of R236fa and CO_2 at T_{sat} = 15°C, which is within the range of the simulation, from -15 to 25°C. The physical properties were obtained from REFPROP version 7.0 [14]. The latent heat of CO_2 is higher than R236fa. The liquid and vapor density ratio of R236fa is much higher than that of CO_2. The liquid viscosity of R236fa is much higher than that of CO_2 and the surface tension of R236 is much higher than that of CO_2. The physical property differences may explain the different heat transfer and two-phase pressure drop behaviours for these two fluids.

Table 2 Physical properties of R236fa and CO_2

Physical properties	R236fa	CO_2
T_{sat} (°C)	15	15
p_{sat} (MPa)	0.19	5.1
ρ_L (kg/m³)	1392.8	821.2
ρ_V (kg/m³)	13.1	160.7
h_{LV} (kg/kJ)	151.6	176.7
μ_L (μPas)	324.3	74.4
μ_V (μPas)	10.5	18.95
σ (N/m)	0.01125	0.00195

Figure 1 shows the variation of exit vapor quality x_e versus saturation temperature T_{sat} for R236fa and CO_2 at a mass flux G = 1500 kg/m²s and a base heat flux q_b = 300 W/cm² (3MW/m²) when they evaporate in the silicon multi-microchannel evaporator in Fig. 1. The local vapor quality x_z at position z along flow direction is determined according to energy balance as

$$x_z = \frac{zq_b}{HGh_{LV}} \qquad (3)$$

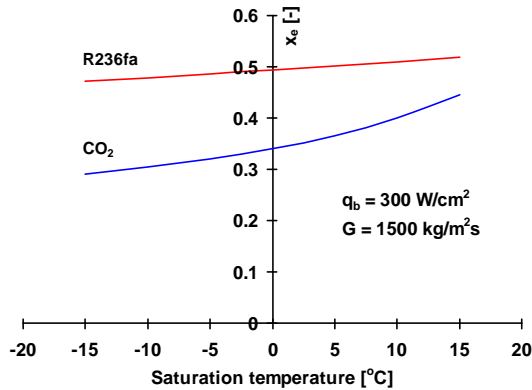The exit vapor quality x_e is thus obtained when $z = L$.

Figure 1 Exit vapour quality x_e versus saturation temperature T_{sat} for R236fa and CO_2 at the indicated conditions

Both the selected mass flux and base heat flux here represent the maximum values used in the present study. It can be seen from Fig. 1 that the exit vapor qualities of CO_2 are much lower than those of R236fa at the same conditions. This is very meaningful when selecting a coolant for cooling

microprocessors using the silicon multi microchannel evaporator because the two-phase pressure drop is directly proportional to x_e.

SIMULATION OF FLOW BOILING HEAT TRANSFER AND TWO-PHASE PRESSURE DROPS OF CO_2

The recent flow boiling heat transfer and two-phase pressure drop models for CO_2 of Cheng et al. [1, 2] are used to simulate the heat transfer and pressure drop behaviors of CO_2 in microchannels with diameters ranging from 0.44 to 1 mm. For non-circular channels, the equivalent diameter D_{eq} should be used in these models. Thus, the microchannels in Fig. 1, with an equivalent diameter D_{eq} = 0.44 mm, is included in the simulations below. It should be pointed out that these models are extrapolated below its minimum diameter limit of 0.6 mm. However, the predicted heat transfer and pressure drop results still show some interesting parametric trends which are helpful in selecting heat transfer coefficients for the simulation of base temperatures of the silicon multi-microchannel evaporator in Fig. 1. No equations of our model are presented here but can be found in [1, 2]. The experimental results for R236fa together with their test conditions and methods can be found in [9].

Simulation Results of CO_2 Flow Boiling Heat Transfer

Figure 3 shows the effect of channel diameter on CO_2 heat transfer. Heat transfer coefficient increases with decreasing channel diameter. However, this variation is not so notable in the selected diameter range of micro-channels.
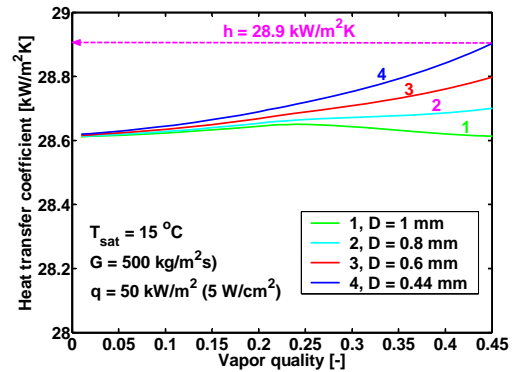

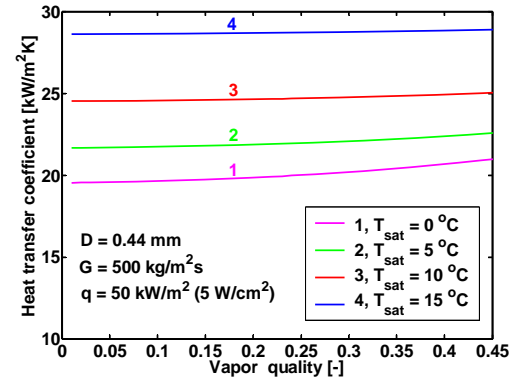**Figure 3** The effect of channel diameter on CO_2 heat transfer

Figure 4 The effect of saturation temperature on CO_2 heat transfer

Figure 4 shows the effect of saturation temperature on CO_2 heat transfer. Heat transfer coefficient increases with increasing saturation temperature from 0 to 15°C. Saturation temperature has a significant effect on heat transfer coefficient.

Figure 5 shows the effect of heat flux on CO_2 heat transfer. The heat transfer coefficient increases strongly with increasing heat flux. Figure 6 shows the effect of mass flux on CO_2 heat transfer. The heat transfer coefficient increases with increasing mass flux, with the variation becoming larger at high vapor qualities. However, the increase of heat transfer coefficient is not so notable in actual percentage terms.
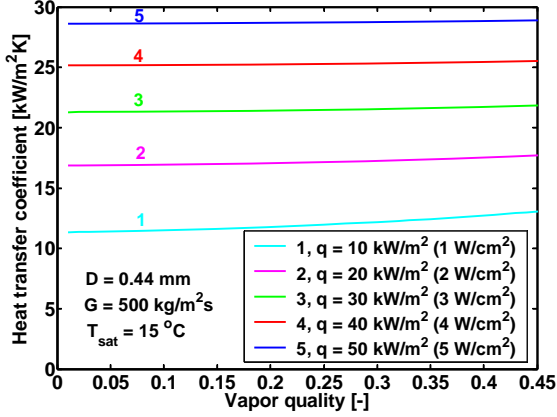
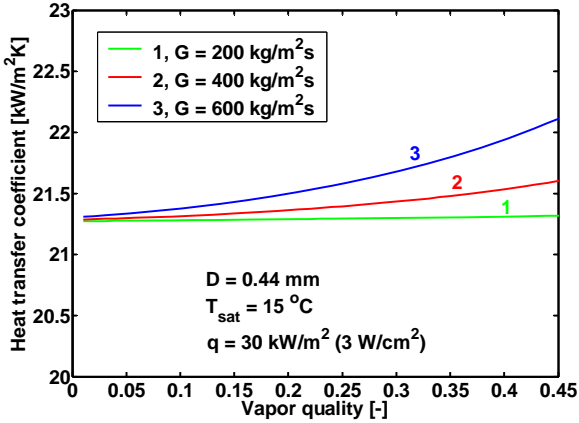**Figure 5** The effect of heat flux on CO_2 heat transfer

Figure 6 The effect of mass flux on heat transfer

Simulation Results of Two-Phase Pressure Drops of CO_2

Figure 7 shows the effect of channel diameter on CO_2 two-phase frictional pressure drop for $G = 1500$ kg/m²s and $T_{sat} = 0$°C. The two-phase frictional pressure drop increases with tube diameter and the diameter effect is significant.

Figure 8 shows the effect of saturation temperature on CO_2 two-phase pressure drop for $G = 1500$ kg/m²s, $D = 0.44$ mm (equivalent diameter of the microchannels in Fig. 1 is used here) and $L = 20$ mm. The two-phase frictional pressure drop decreases with saturation temperature. The effect of saturation temperature becomes significant at high vapor qualities.

Figure 9 shows the effect of mass flux on CO_2 two-phase frictional pressure drop $D = 0.44$ mm, $T_{sat} = 0$°C and $L = 20$ mm. The two-phase frictional pressure drop increases with mass flux.
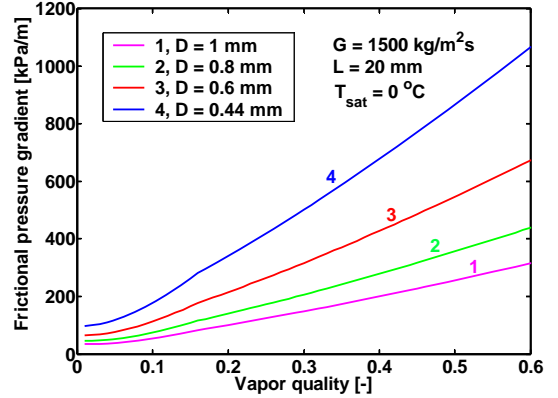

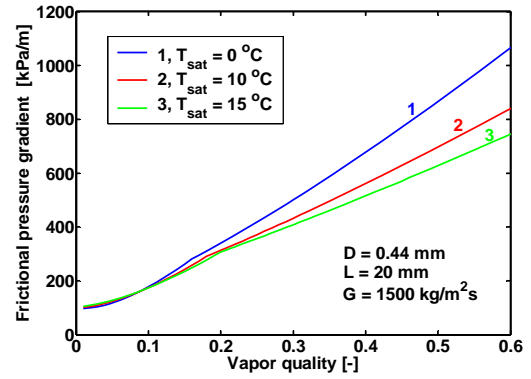**Figure 7** The effect of channel diameter on CO_2 two-phase pressure drop

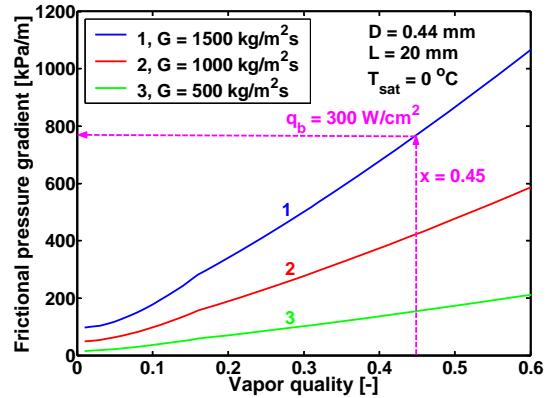**Figure 8** The effect of saturation temperature on CO_2 two-phase pressure drop

Figure 9 The effect of mass flux on CO_2 two-phase pressure drop

The total two-phase pressure drop Δp_{total} for horizontal channel equals two-phase frictional pressure drop Δp_f plus acceleration pressure drop Δp_a as

$$\Delta p_{total} = \Delta p_f + \Delta p_a \qquad (4)$$

$$\Delta p_a = G^2 \left\{ \left[\frac{(1-x)^2}{\rho_L(1-\varepsilon)} + \frac{x^2}{\rho_V \varepsilon} \right]_{out} - \left[\frac{(1-x)^2}{\rho_L(1-\varepsilon)} + \frac{x^2}{\rho_V \varepsilon} \right]_{in} \right\} \quad (5)$$

where void fraction ε is calculated with the Rouhani and Axelsson [15] correlation as

$$\varepsilon = \frac{x}{\rho_V} \left[\left(1+0.12(1-x)\right)\left(\frac{x}{\rho_V} + \frac{1-x}{\rho_L}\right) + \frac{1.18(1-x)\left[g\sigma(\rho_L-\rho_V)\right]^{1/4}}{G\rho_L^{1/2}} \right]^{-1} \quad (6)$$

From the simulated pressure drop results, it may be concluded that a high saturation temperature and a low mass flux should be selected to obtain low pressure drops, so as to reduce the pumping power for a fixed channel diameter. In the case of a base heat flux $q_b = 300$ W/cm^2 (3MW/m^2) and a mass flux $G = 1500$ kg/m^{2}s indicated by the dashed line in Fig. 9, this results in an exit vapor quality of 0.45, the frictional pressure gradient is 780 kPa/m. This corresponds to a frictional pressure drop less than 16 kPa for the microchannel length $L = 20$ mm. Considering the accelerational pressure drop Δp_a evaluated by Eq. (5) (about one-third of the two-phase frictional pressure drop), the total two-phase pressure drop Δp_{total} evaluated by Eq. (4) in a single microchannel is less than 25 kPa, which is much less than that for R236fa (162 kPa evaluated by the homogeneous model [9]). Thus, using CO$_2$ requires much less pumping power than R236fa for the same conditions.

SIMULATED BASE TEMPERATURES IN A MULTI-MICROCHANNEL EVAPORATOR

Simulations of base temperature of the silicon multi-microchannel evaporator in Fig. 1 have been performed. First, wall heat fluxes q_W were assumed to predict the flow boiling heat transfer coefficients of CO$_2$ for certain conditions. Then, Eq. (7) was used to determine the wall temperature T_W. Finally, Eqs. (8) to (12) were iteratively solved to obtain the base temperatures. The heat transfer coefficient was defined as

$$h = \frac{q_W}{T_W - T_{sat}} \quad (7)$$

and the base heat flux was evaluated as [16]:

$$q_b = q_W \frac{W + 2\eta H}{W + t} \quad (8)$$

where the fin efficiency was calculated as follows [16]:

$$\eta = \frac{\tanh(mH)}{mH} \quad (9)$$

$$m = \sqrt{\frac{h(W+L)}{k_{si}WL}} \quad (10)$$

The thermal conductivity of silicon was calculated as in [9]:

$$k_{si} = 0.0018T^2 - 0.7646T + 143.25 \quad (11)$$

The base temperature was calculated with a one dimensional heat conduct model as

$$T_b = T_W - \frac{q_b e}{k_{si}} \quad (12)$$

Figure 10 shows the simulated base temperatures of CO$_2$ flow boiling in the silicon multi-microchannel evaporator at three different saturation temperatures and a mass flux of 1000

kg/m^{2}s. It can be seen that a lower saturation temperature can contribute to lower base temperatures. However, in practical applications, the higher energy cost caused by using a lower temperature should be considered.
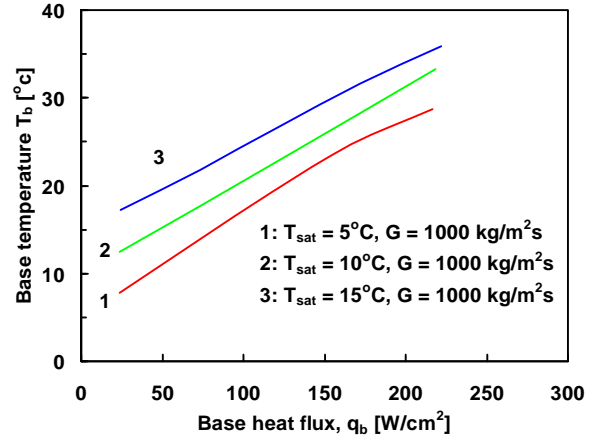

Figure 10 Simulation of base temperatures of CO$_2$ for different saturation temperatures at a fixed mass flux
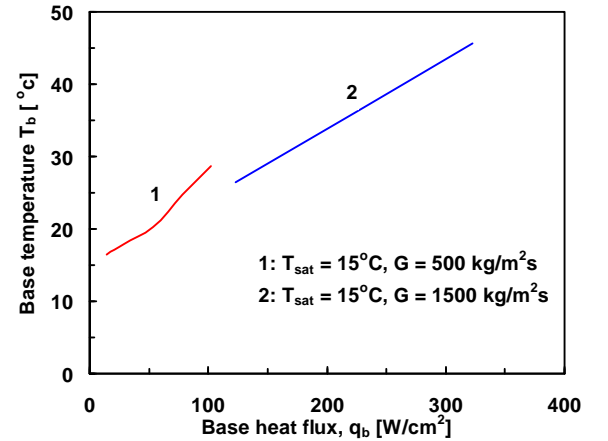

Figure 11 Simulation of base temperature of CO$_2$ for two different mass fluxes at a fixed saturation temperature

Figure 11 shows the simulated base temperatures of CO$_2$ flow boiling in the silicon multi-microchannel evaporator at mass fluxes of 500 kg/m^{2}s and 1500 kg/m^{2}s and at a saturation temperature of 15°C. With the higher mass flux, a higher base heat flux may be cooled. For the lower mass flux, a more limited heat flux may be dissipated by the evaporator because of the limitation of the exit vapor quality x_e. For the lower mass flux at higher heat flux, the exit vapor quality may reach 1 and thus cooling is no longer effective.

Figure 12 shows the comparison of the simulated base temperatures of CO$_2$ and R236fa flow boiling in the silicon multi-microchannel evaporator at a mass flux of 987.6 kg/m^{2}s and a saturation temperature of 25°C for base heat fluxes in the range from 20 to 100 W/cm^2. It can be seen that CO$_2$ can achieve lower base temperatures than R236fa by 4 to 6 K.
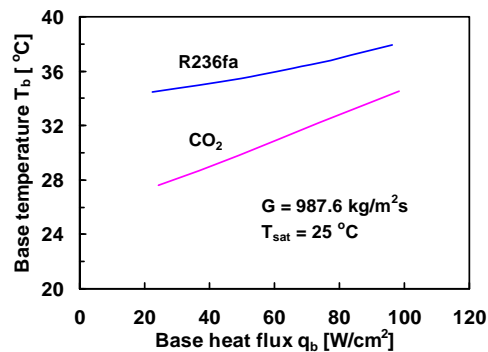
Figure 12 Comparisons of simulation results of base temperature of CO_2 and R236fa at the indicated conditions

It should however be pointed out that very high heat flux cooling is beyond the applicable conditions of the CO_2 models. In the simulations, heat transfer coefficients at much lower heat fluxes (less than $5 W/cm^2$) were used in the simulation. This makes the simulated results much more conservative. However, further experiments are needed for CO_2 flow boiling in microchannels to extend the heat transfer model to extremely high heat fluxes and to understand the physical mechanisms which might be quite different from those in macro-scale channels. Apparently, no such information is available so far.

Although CO_2 has much better thermal performance and much lower pumping power requirements than R236fa, it must be realized that the operational pressure of CO_2 is much higher than R236fa. Therefore, CO_2 also presents a great technological challenge like other new cooling technology.

CONCLUSIONS

In this study, simulations of the base temperatures of a silicon multi-microchannel evaporator using CO_2 for evaporation were performed for q_b = 20-100 W/cm^2, G = 987.6 kg/m^2s and T_{sat} = 25°C. It shows that the base temperatures using CO_2 are 4-6 K lower than those using R236fa. CO_2 has much higher heat transfer coefficients and lower pressure drops in the multi-microchannel evaporator than R236fa. However, the operational pressure of CO_2 is much higher than that of R236fa. Based on the analysis and comparison, CO_2 appears to be a promising coolant for microprocessors for low temperature applications. Further study on the application of CO_2 flow boiling for chip cooling should be investigated.

REFERENCES

[1] Cheng L., Ribatski G., Moreno Quibén J., and Thome J.R., New prediction methods for CO_2 evaporation inside tubes: part I — a general two-phase flow pattern map and development of a phenomenological model of two-phase flow frictional pressure drop, Int. J. Heat Mass Transfer, 51 (2008) 111-124.

[2] Cheng L., Ribatski G., and Thome J.R.,L. Cheng, G. Ribatski, J.R. Thome, New prediction methods for CO_2 evaporation inside tubes: part II — a general flow boiling heat transfer model based on flow patterns, Int. J. Heat Mass Transfer, 51 (2008) 125-135.

[3] Thome, J.R., Recent advances in thermal modeling of micro-evaporators for cooling of microprocessors, ASME International Mechanical Engineering Congress and Exhibition (IMECE), Seattle, Nov. 10-16. 2007.

[4] Thome, J.R., Revellin, R., Agostini, B., and Park, J.E., Cooling of microprocessors using flow boiling of refrigerants in micro-evaporators, International Symposium on Phase Change, UK Heat Transfer 2007, Edinburgh, Scotland, Sept. 12. 2007.

[5] Tuckerman, D.B., and Pease, R.F.W., High performance heat-sinking for VLSI, IEEE Electron Device Lett. 2 (1981) 126-129.

[6] Hetsroni, G., Mosyak, A., Segal, Z., and Ziskind, G., A uniform temperature heat sink for cooling of electronic devices, Int. J. Heat Mass Transfer 45 (2002) 3275-3286.

[7] Lee, J., and Mudawar I., Two-phase flow in high-heat-flux micro-channel heat sink for refrigeration cooling applications: part I-pressure drop characteristics, Int. J. Heat Mass Transfer 48 (2005) 928-940.

[8] Lee, J., and Mudawar I., Two-phase flow in high-heat-flux micro-channel heat sink for refrigeration cooling applications: part II-heat transfer characteristics, Int. J. Heat Mass Transfer 48 (2005) 941-955.

[9] Agostini, B., Thome, J.R., Fabbri, M., Calmi, D., Kloter, U. and Michel, B., (2007). High heat flux flow boiling in silicon multi-microchannels: Part I – heat transfer characteristics of R-236fa, *Int. J. Heat Mass Transfer*, in press.

[10] Agostini, B., Thome, J.R., Fabbri, M., Calmi, D., Kloter, U. and Michel, B., (2007). High heat flux flow boiling in silicon multi-microchannels: Part II – heat transfer characteristics of R-245fa, *Int. J. Heat Mass Transfer*, in press.

[11] J.R. Thome, J.R., and Ribatski, G., State-of-the art of flow boiling and two-phase flow of CO_2 in macro- and micro-channels, Int. J. Refrigeration 28 (2006) 1149-1168.

[12] Cheng, L., Ribatski, G., Wojtan, L., and Thome, J.R., New flow boiling heat transfer model and flow pattern map for carbon dioxide evaporating inside tubes, Int. J. Heat Mass Transfer 49 (2006) 4082-4094.

[13] Cheng, L., Ribatski, G., Wojtan, L., and Thome, J.R., Erratum to: New flow boiling heat transfer model and flow pattern map for carbon dioxide evaporating inside tubes, [Heat Mass Transfer 49 (21-22) (2006) 4082-4094], Int. J. Heat Mass Transfer 50 (2007) 391.

[14] REFPROP. NIST Refrigerant Properties Database 23, Gaithersburg, MD, 2002, Version 7.0.

[15] Rouhani, Z., and Axelsson, E., Calculation of volume void fraction in a subcooled and quality region, Int. J. Heat Mass Transfer 17 (1970) 383-393.

[16] Incropera, F.P., and Dewitt, D.P., Fundamental of Heat and Mass Transfer, 5th ed., Wiley, New York, 2002.